

# Novel Pyrazole Derivatives Effectively Inhibit Osteoclastogenesis, a Potential Target for Treating Osteoporosis

Ting-Hao Kuo,<sup>†</sup> Tzu-Hung Lin,<sup>†</sup> Rong-Sen Yang,<sup>§</sup> Sheng-Chu Kuo,<sup>||</sup> Wen-Mei Fu,<sup>\*,†,‡</sup> and Hsin-Yi Hung<sup>\*,‡,‡</sup>

<sup>†</sup>Pharmacological Institute and <sup>‡</sup>Drug Research Center, College of Medicine, National Taiwan University, Taipei, 100, Taiwan

<sup>§</sup>Department of Orthopedics, College of Medicine, National Taiwan University Hospital, Taipei 100, Taiwan

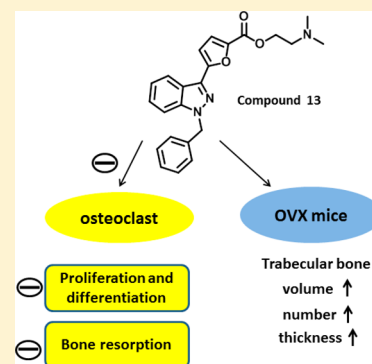
<sup>||</sup>Graduate Institute of Pharmaceutical Chemistry, China Medical University, Taichung, 404, Taiwan

<sup>‡</sup>Chinese Medicine Research and Development Center, China Medical University Hospital, Taichung, 404, Taiwan

<sup>#</sup>School of Pharmacy, National Cheng Kung University Hospital, College of Medicine, National Cheng Kung University, Tainan, 701, Taiwan

## Supporting Information

**ABSTRACT:** As human beings live longer, age-related diseases such as osteoporosis will become more prevalent. Intolerant side effects and poor responses to current treatments are observed. Therefore, novel effective therapeutic agents are greatly needed. Here, pyrazole derivatives were designed and synthesized, and their osteoclastogenesis inhibitory effects both *in vitro* and *in vivo* were evaluated. The most promising compound 13 with a 2-(dimethylamino)ethyl group inhibited markedly *in vitro* osteoclastogenesis as well as the bone resorption activity of osteoclasts. Compound 13 affected osteoclast's early proliferation and differentiation more than later fusion and maturation stages. In ovariectomized (OVX) mice, compound 13 can inhibit the loss of trabecular bone volume, trabecular bone number, and trabecular thickness. Moreover, compound 13 can antagonize OVX-induced reduction of serum bone resorption marker and then compensatory increase of the bone formation marker. To sum up, compound 13 has high potential to be developed into a novel therapeutic agent for treating osteoporosis in the future.



## INTRODUCTION

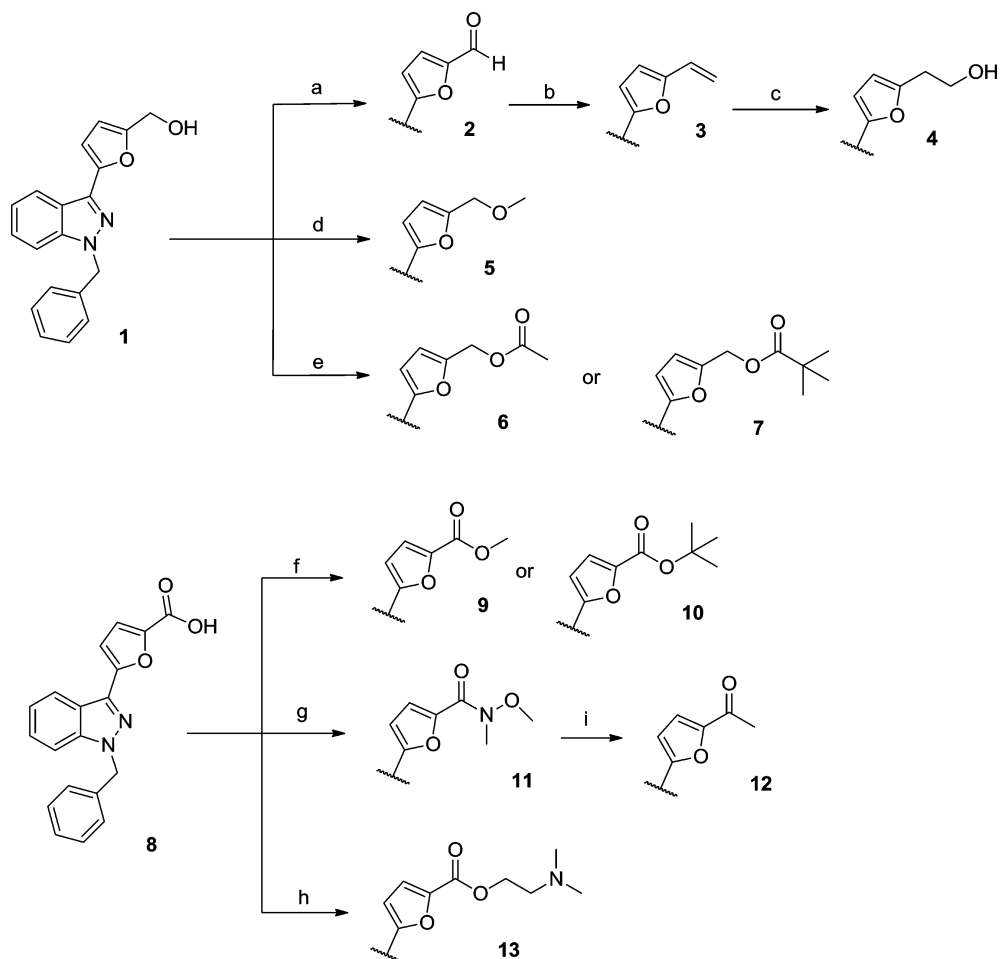
With the increase in aging populations, fracture rates accompanying urbanization also increase. In the United States, the population with an elevated risk of osteoporotic fracture contains an estimated 19% of older men and 30% of older women, which is similar in Europe and is projected to rise worldwide.<sup>1–3</sup> Remaining challenges in implementing therapy for osteoporosis still occur, even though the diagnosis is made and a decision is made regarding treatment, which largely result from bad compliance, intolerable side effects, and inadequate response to current therapeutic agents.<sup>4</sup> Therefore, new therapeutic agents for treating osteoporosis are still a huge need.

The homeostasis of bone metabolism consists of a continuously balanced remodeling process by two opposed forces: bone resorption and bone formation. Osteoclasts derived from hematopoietic stem cells play an important role in bone resorption, and osteoblasts derived from mesenchymal stem cells mediate the main part in bone formation or the so-called bone mineralization. Imbalance actions between osteoclasts and osteoblasts will cause lots of metabolic bone disorders, such as osteoporosis resulting from increased osteoclast activity and decreased osteoblast activity.<sup>5,6</sup> To date, many studies have suggested that osteoblasts play a role

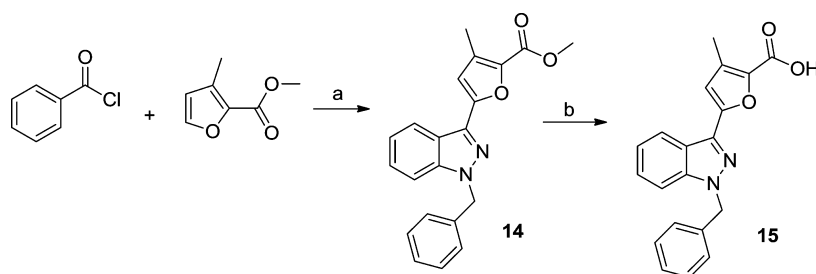
not only in bone formation but also in osteoclast maturation and bone resorption. Osteoclast formation starts from a monocyte progenitor and requires the presence of a receptor activator of nuclear factor kappa-B ligand (RANKL) and a macrophage colony-stimulating factor (M-CSF). Interaction between RANKL expressed on an osteoblast and RANK expressed on an osteoclast precursor activates RANKL–RANK signaling to induce bone resorption via the NF- $\kappa$ B pathway. However, M-CSF, which is released from osteoblasts, acts via the colony-stimulating factor 1 receptor on the osteoclast precursor and leads to the differentiation of osteoclasts from monocyte/macrophage.<sup>7–9</sup>

Since osteoclastogenesis is critical for bone resorption, many pharmacological agents aim to suppress RANKL-induced osteoclastogenesis, such as hormone replacement therapy and bisphosphonates like alendronate and denosumab, a human monoclonal antibody against RANKL.<sup>10</sup> However, there are intolerable side effects and inadequate response to current therapeutic agents. A new therapeutic direction was found by the studies on a nitric oxide (NO) donor for the treatment of osteoporosis. Clinical data were retrieved from women taking

Received: December 29, 2014

Scheme 1. Synthesis of Pyrazole Derivatives 2–7 and 9–13<sup>a</sup>

<sup>a</sup>Reagent and conditions: (a) PDC, CH<sub>2</sub>Cl<sub>2</sub>; (b) H<sub>3</sub>C-PPh<sub>3</sub>Br, tBuOK, THF; (c) (i) BH<sub>3</sub>-SMe<sub>2</sub>, THF, 0 °C, N<sub>2</sub>; (ii) NaOH, H<sub>2</sub>O<sub>2</sub>, 0 °C → r.t.; (d) NaH, CH<sub>3</sub>I, CH<sub>2</sub>Cl<sub>2</sub>; (e) Ac<sub>2</sub>O, reflux for 6, *t*-BuOH, (COCl)<sub>2</sub>, CH<sub>2</sub>Cl<sub>2</sub> for 7; (f) EDCl, DMAP, MeOH for 9, *t*-BuOH for 10; (g) EDCl, HOBT, NEM, CH<sub>3</sub>NHOCH<sub>3</sub>; (h) (i) (COCl)<sub>2</sub>, CH<sub>2</sub>Cl<sub>2</sub>, N<sub>2</sub>; (ii) HOCH<sub>2</sub>CH<sub>2</sub>N(CH<sub>3</sub>)<sub>2</sub>, CH<sub>2</sub>Cl<sub>2</sub>; (i) CH<sub>3</sub>MgBr, CH<sub>2</sub>Cl<sub>2</sub>.

Scheme 2. Synthesis of Pyrazole Derivatives 14–15<sup>a</sup>

<sup>a</sup>Reagent and conditions: (a) (i) FeCl<sub>3</sub>, CH<sub>2</sub>Cl<sub>2</sub>, ClCH<sub>2</sub>CH<sub>2</sub>Cl, reflux; (ii) PhCH<sub>2</sub>NHNH<sub>2</sub>·2HCl, NaOAc, MeOH; (iii) Pb(OAc)<sub>4</sub>, BF<sub>3</sub>·Et<sub>2</sub>O, CH<sub>2</sub>Cl<sub>2</sub>, 0 °C; (b) KOH, MeOH.

organic nitrates, and the results showed nitrite use was associated with increased bone mineral density (BMD) and lower risk of hip fracture.<sup>11,12</sup> 3-(5'-Hydroxymethyl-2'-furyl)-1-benzyl indazole is well-known for the NO-dependent soluble guanylyl cyclase (sGC) activator and subsequently increasing cyclic guanosine monophosphate (cGMP) formation.<sup>13</sup> Inspired by the studies above, we thus aim to discover a potential osteoclastogenesis inhibitor by screening a series of small molecules with the core structure of 3-(5'-hydroxymethyl-2'-

furyl)-1-benzyl indazole to study the structure–activity relationship, action mechanism, and *in vivo* effects.

## RESULTS AND DISCUSSION

**Chemistry.** The relationship between pyrazole structure and antiosteoporosis activity is largely undefined. Therefore, diversified pyrazole derivatives were designed and synthesized. As shown in Scheme 1, 3-(5'-hydroxymethyl-2'-furyl)-1-benzyl indazole (1) or 5'-carboxylic acid derivative (8) (courtesy of Yungshin Pharm Ind. Co. Ltd.) were used as starting materials.

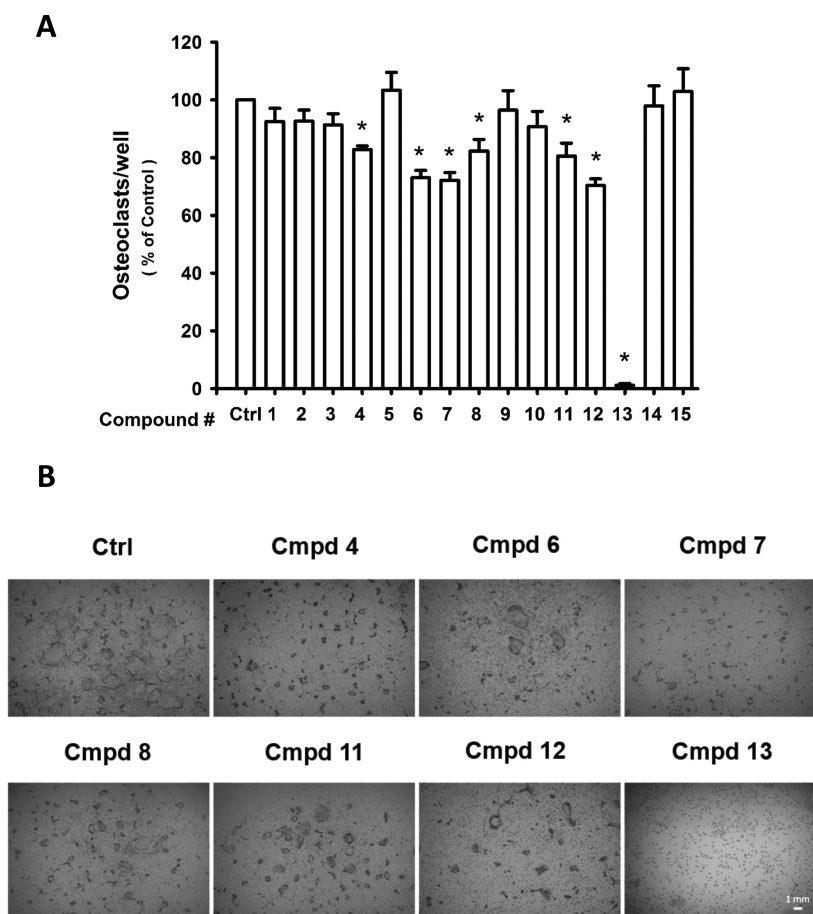


**Figure 1.** Inhibition of osteoclastogenesis by pyrazole derivatives. (A) Bone marrow-derived preosteoclasts from male rats were seeded in 24 wells. Different derivatives were added in the presence of 50 ng/mL RANKL and 20 ng/mL M-CSF for 5 days. TRAP staining was then performed. Nuclei greater than 3 were counted as osteoclasts. The representative images are shown in B. Data are presented as the mean  $\pm$  SEM ( $N = 6$ ), \*,  $p < 0.05$  as compared with the Ctrl (control).

Pyridium dichromate oxidation was applied, and 5'-carbaldehyde derivative **2** was obtained.<sup>14</sup> The Wittig reaction using methyltriphenylphosphonium bromide and potassium *tert*-butoxide as base was given 5'-vinyl derivative **3**. Hydroboration–oxidation was applied and 5'-hydroxyethyl derivative **4** was obtained. Methoxymethyl derivative **5** was obtained by treating **1** with sodium hydride and iodomethane.<sup>15</sup> Esterification with acetic anhydride or oxalyl chloride and *tert*-butanol was given **6** or **7**, respectively.<sup>16</sup> Reverse ester linkage derivatives were synthesized using *N*-(3-(dimethylamino)propyl)-*N'*-ethylcarbodiimide hydrochloride (EDCI), DMAP, and methanol for **9** or *tert*-butanol for **10**.<sup>15,17</sup> Weinreb amide derivative **11** was easily obtained in high yield using EDCI, 1-hydroxybenzotriazole hydrate (HOBt), and *N,O*-dimethylhydroxylamine. 5'-Ethanone derivative **12** was obtained via methylmagnesium bromide substitution. Compound **13** was synthesized from compound **8**. Under inert atmosphere, oxalyl chloride (10 equiv) was added to compound **8** (1 equiv) in anhydrous dichloromethane at 0 °C to form an acyl chloride intermediate. Excess oxalyl chloride was evaporated, and *N,N*-dimethylethanolamine (3 equiv) was then added to the reaction mixture to give compound **13**.

3-(5'-Hydroxymethyl-2'-furyl)-1-benzyl indazole was easily metabolized by liver microsomal enzymes (unpublished data). Therefore, methyl substitution on the 4' position was designed to reduce the first-pass effect. The synthetic procedure is shown

in Scheme 2. Benzyl chloride and methyl 3-methyl-2-furoate were used as starting materials and underwent Friedel–Crafts acylation using an iron(III) chloride as catalyst. The corresponding ketone went through a condensation reaction with benzylhydrazine. Finally, cyclization was done by treating  $\text{Pb}(\text{OAc})_4$  and then  $\text{BF}_3 \cdot \text{Et}_2\text{O}$  to yield methyl 5-(1'-benzyl-1*H*-indazol-3'-yl)-3-methylfuran-2-carboxylate (**14**).<sup>18</sup> Carboxylic acid derivative **15** was simply obtained by potassium hydroxide reflux with **14**.

**Inhibition of Osteoclastogenesis by Pyrazole Derivatives.** In order to quickly obtain a structure–activity relationship, diversified pyrazole derivatives including ester, acid, aldehyde, alcohol, alkene, and amide were chosen for screening osteoclastogenesis inhibitory activity. Each derivative was added to bone marrow-derived preosteoclasts (from male rats) to examine the inhibitory activity on osteoclastogenesis in 24 wells. Different testing compounds at 10  $\mu\text{M}$  were added in the presence of RANKL (50 ng/mL) and M-CSF (20 ng/mL) for 5 days. After 5 days, tartrate resistant acid phosphatase-stain (TRAP-stain) was used to confirm osteoclast formation. Both TRAP-positive and nuclei  $\geq 3$  cells were counted. Compounds **4**, **6**, **7**, **8**, **11**, and **12** were found to reduce 20–25% of osteoclast formation compared with that of the vehicle (Ctrl) (Figure 1A), and the representative images are shown in Figure 1B. However, compound **13** markedly inhibited osteoclast formation over 90% (Figure 1A and B). Taken together, these

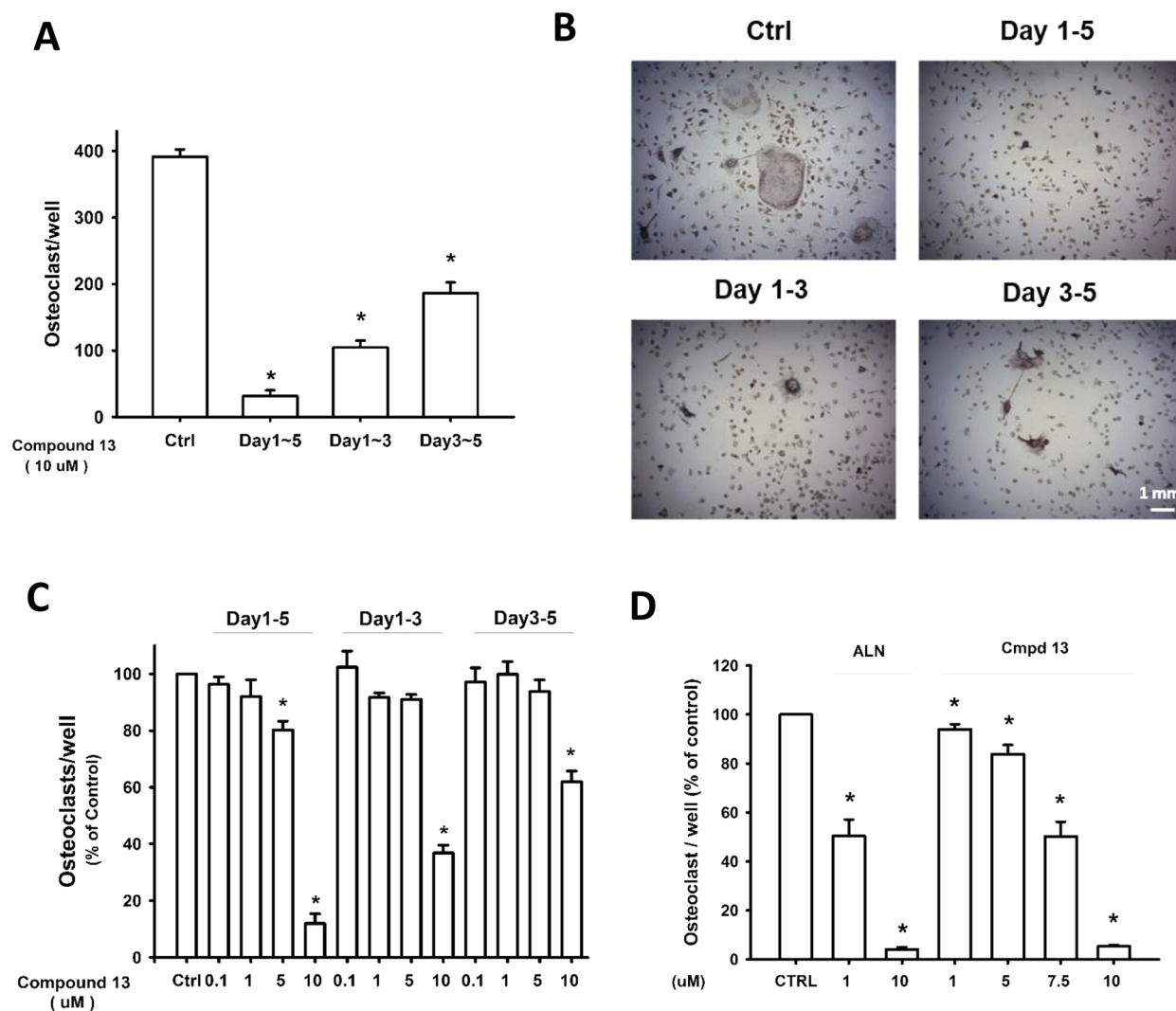


**Figure 2.** Inhibition of osteoclastogenesis by compound 13. Bone marrow-derived preosteoclasts from male rats were seeded in 24 wells. (A) Compound 13 was added in different days in the presence of 50 ng/mL RANKL and 20 ng/mL M-CSF. Note that compound 13 (10 μM) markedly inhibited osteoclastogenesis when incubated on days 1–5 ( $N = 3$ ). The representative images are shown in B. (C) Compound 13 inhibited osteoclastogenesis in a concentration-dependent manner ( $N = 3$ ). (D) Compared with alendronate (ALN), compound 13 had similar inhibitory action at 10 μM on osteoclastogenesis ( $N = 4$ ). Data are presented as the mean  $\pm$  SEM, \*,  $p < 0.05$  as compared with the Ctrl (control).

results suggest that the derivatives with a core structure of 3-(5'-hydroxymethyl-2'-furyl)-1-benzylindazole can inhibit osteoclastogenesis. Compared with compounds 6, 7, 9, and 10, the order of the ester bond seems to be important for activity. From compounds 1 and 4, we can see that one more carbon contributes some effects to the activity. Moreover, a longer chain with more heteroatoms such as 4 and 13 seems to exert more potent inhibitory activity. Among all of the compounds, compound 13 with the 2-(dimethylamino)ethyl group was the most potent.

#### Inhibition of Osteoclastogenesis and the Bone Resorption Activity of Osteoclasts by Compound 13.

To our current knowledge, two phases are involved in osteoclast formation: the early phase of proliferation and differentiation and the late phase of fusion and maturation.<sup>8,19</sup> Therefore, compound 13 was chosen to study the mechanism of the inhibition of osteoclastogenesis. In the presence of 50 ng/mL RANKL and 20 ng/mL M-CSF for 5 days, day 1 to day 3 was defined as the early phase, and compound 13 was added on day 1. However, day 3 to day 5 was defined as the late phase,

and compound 13 was added on day 3. After 5 days, the result showed that compound 13 inhibited two phases but exerted much stronger effects in early phase than in late phase (Figure 2A), and the representative images are shown in Figure 2B. Compound 13 exerted concentration-dependent inhibition of osteoclastogenesis (Figure 2C). In addition, compound 13 exerted inhibitory activity in osteoclastogenesis similar to that of alendronate (ALN) at 10 μM (Figure 2D). It was also found that compound 13 at 10 μM had no cytotoxicity in primary preosteoclasts (Figure S1, Supporting Information).

It is well known that mature osteoclasts play an important role in bone resorption. As compound 13 markedly inhibits osteoclastogenesis, we next examined whether compound 13 inhibited the function of osteoclasts. Preosteoclasts were seeded in Osteo Assay Plate (Corning, USA) in the presence of 50 ng/mL RANKL and 20 ng/mL M-CSF for the resorption assay. After 5 days of culture, compound 13 was then added for another 3 days. It was found that compound 13 inhibited the resorption area of osteoclasts over 75% (Figure 3A and B). There was no significant difference in osteoclastic number

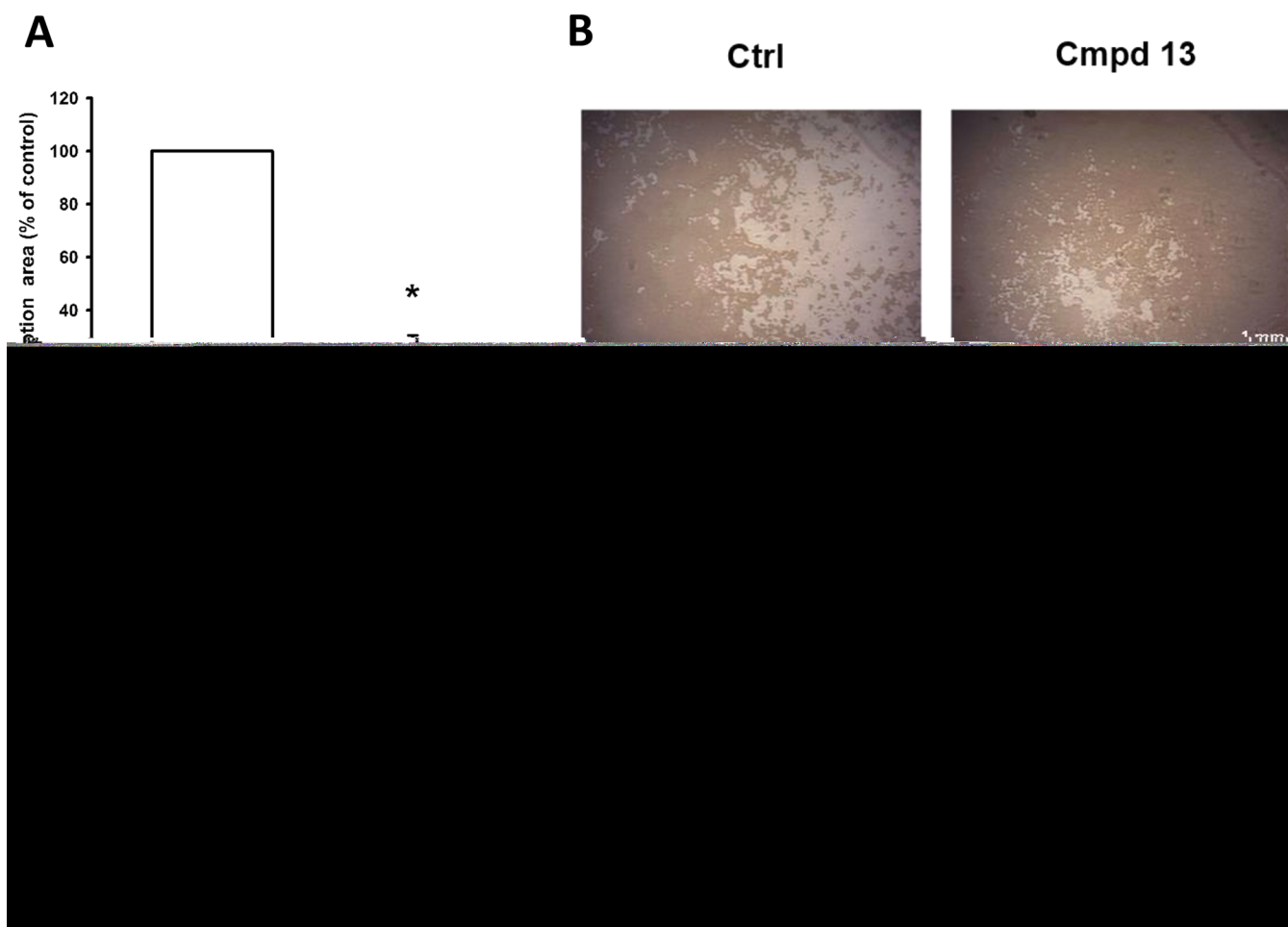


**Figure 3.** Inhibition of bone resorption activity of osteoclasts by compound 13. Bone marrow-derived preosteoclasts were seeded in Osteo Assay Plate 24 wells (Corning, USA) in the presence of 50 ng/mL RANKL and 20 ng/mL M-CSF for 5 days. RANKL and M-CSF were then removed, and compound 13 (10  $\mu$ M) was added for another 3 days. (A) Compared with the control, compound 13 significantly inhibited the resorption activity of osteoclasts ( $N = 4$ ). The representative images are shown in B. (C) There was no significant difference in osteoclast number on day 8 between the control and compound 13 ( $N = 4$ ). The representative images are shown in D. Data are presented as the mean  $\pm$  SEM, \*,  $p < 0.05$  as compared with the Ctrl (control).

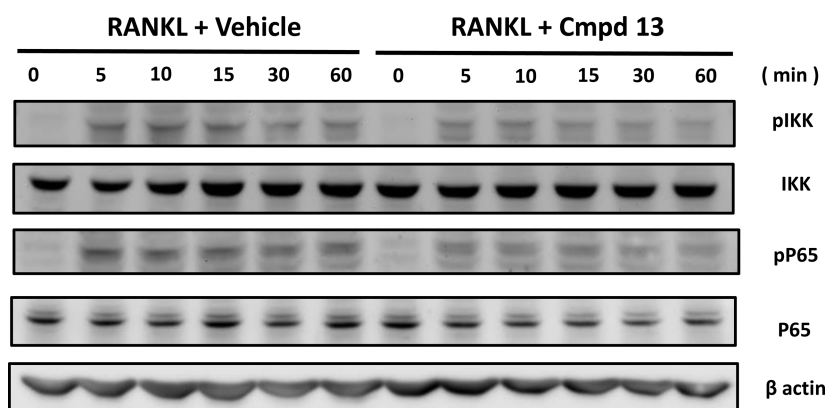


**Figure 4.** Inhibition of RANKL-induced NF- $\kappa$ B activation in RAW264.7 cells by compound 13. RAW264.7 cells were treated with RANKL (50 ng/mL) for several time intervals. Western blot analysis revealed that treatment with RANKL increased the phosphorylation of IKK and P65 beginning from 5 min. Pretreatment with compound 13 (10  $\mu$ M) markedly inhibited RANKL-induced phosphorylation of IKK and P65.

between the control and compound 13 on day 8 (Figure 3C and D). These results indicate that compound 13 also exerted direct bone resorption inhibitory activity.

Moreover, we also used bone marrow-derived preosteoclasts from male ICR mice to examine the effect of compound 13 on

osteoclastogenesis. As shown in Figure S2 (Supporting Information), compound 13 (10  $\mu$ M) also exerted marked inhibition on osteoclastogenesis. We also examined the effect of pyrazole compounds on bone nodule formation of osteoblasts. Compound 13 did not exert inhibitory action on osteoblasts

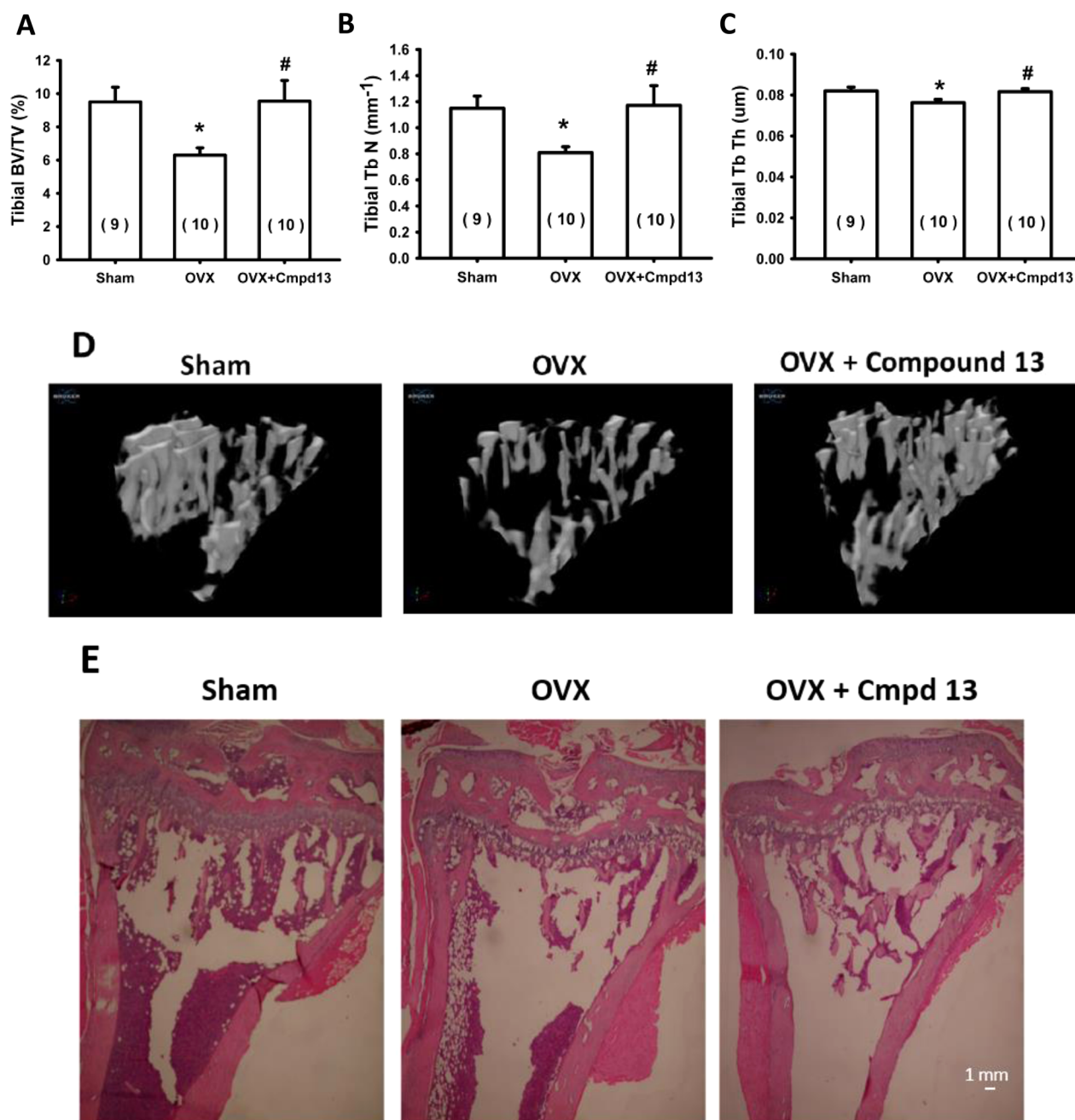


**Figure 5.** Compound 13 inhibits ovariectomy (OVX)-induced bone loss in tibia. Female mice were ovariectomized. Compound 13 (Cmpd 13) was administered at 10 mg/kg (s.c.), 5 days/week. Tibiae were removed from mice on day 30 and fixed in 4% paraformaldehyde, and  $\mu$ CT analysis was then performed. Note that compound 13 antagonized OVX-induced reduction of bone volume (A) and the decrease of trabecular bone number (B) and trabecular thickness (C). Radiographs are shown in D. (E) H&E staining was performed. Note that OVX reduced the trabecular number, which was antagonized by compound 13 treatment. Data are presented as the mean  $\pm$  SEM ( $N = 9 \sim 10$ ), \*,  $p < 0.05$  as compared with Sham. #,  $p < 0.05$  as compared with the OVX group.

(Figure S3A, Supporting Information). Furthermore, compound 13 had no effect on the cell viability of osteoblasts (Figure S3B, Supporting Information). To sum up, compound 13 significantly inhibited osteoclastogenesis and the bone resorption activity of osteoclasts and had no effect on the bone nodule formation of osteoblasts.

**Compound 13 Inhibits RANKL-Induced NF- $\kappa$ B Activation.** Since the NF- $\kappa$ B pathway plays an important role in RANKL-RANK signaling, we then examined the potential mechanisms of compound 13 on the NF- $\kappa$ B signaling pathway. Since we have found that compound 13 also inhibited

osteoclast formation in macrophage-like RAW 264.7 cells (data not shown), we then used RAW cells to investigate the effect of compound 13 on NF- $\kappa$ B signaling. RAW cells were treated with RANKL at 50 ng/mL to activate NF- $\kappa$ B signaling. RANKL rapidly phosphorylated the inhibitor of  $\kappa$ B kinase (Ikk) and also P65. As shown in Figure 4, significant phosphorylation of IKK and P65 was observed within 15 min following the treatment of RANKL. Compound 13 at 10  $\mu$ M significantly inhibited RANKL-induced NF- $\kappa$ B activation. Therefore, the decrease of the RANKL-induced NF- $\kappa$ B pathway may be

involved in the inhibitory action of compound 13 in osteoclastogenesis.

**Compound 13 Inhibits Osteoporosis in Ovariectomized OVX Mice.** Ovariectomy (OVX) in female rodents is a well-established animal model in osteoporosis. OVX mice were characterized by remarkably decreased trabecular bone volume relative to the tissue volume (BV/TV %), trabecular bone number (Tb.N), and trabecular thickness (Tb.Th) in tibiae compared with those sham-operated (Sham) mice.<sup>19</sup> Compound 13 was evaluated for its potency against osteoporosis *in vivo* using bilateral ovariectomy and sham-operated female ICR mice (12 weeks-old). Two days after surgery, the mice were subcutaneously injected with compound 13 (10 mg/kg, 5 days/week) or vehicle for 30 days. After 30 days, tibiae were taken out from mice and fixed in 4% paraformaldehyde and microcomputed tomography ( $\mu$ -CT) analysis was then performed. BV/TV %, Tb.N, and Tb.Th were used as the osteoporosis parameters. Our findings revealed that BV/TV, trabecular bone number, and trabecular thickness were more significantly reduced, which were antagonized by compound 13 treatment (Figure 5A–D). H&E staining was also performed. It was also found that the trabecular bone decreased in OVX mice, which was antagonized by compound 13 treatment (Figure 5E).

**Compound 13 Antagonizes OVX-Induced Change of Serum Bone Resorption and Bone Formation Markers.** Ovariectomized and sham-operated female ICR mice were sacrificed on day 30, and blood samples were collected for analysis. A RatLaps EIA kit was used to detect the serum level of C-terminal telopeptides of type-I collagen (CTx), a bone resorption marker (Figure 6A). A Rat-MID osteocalcin EIA kit was used to detect the serum level of osteocalcin, a bone formation marker (Figure 6B). It was found that ovariectomy increased both serum markers of CTx and osteocalcin, which can be significantly antagonized by compound 13.

## CONCLUSIONS

With the aging of the population, diseases related with aging such as osteoporosis will become more and more critical. Patients suffer intolerable side effects and poor responses to current treatments. Therefore, novel and effective therapeutic agents are in great need. Here, a series of pyrazole derivatives were designed, synthesized, and evaluated for their osteoclastogenesis inhibitory effects both *in vitro* and *in vivo*. The most promising compound 13 with the 2-(dimethylamino)ethyl group showed significant *in vitro* osteoclastogenesis inhibitory effects and retainment of BV/TV, trabecular bone number, and trabecular thickness in OVX mice. Moreover, compound 13 affected osteoclast proliferation and differentiation more than later fusion and maturation stages. In addition, compound 13 also exerted inhibitory action on the bone resorption activity of osteoclasts. From serum analysis in OVX mice, compound 13 can antagonize OVX-induced reduction of serum bone resorption markers and then compensatory increase of bone formation markers. To sum up, compound 13 has high potential to be developed as a novel therapeutic agent for treating osteoporosis in the future.

## EXPERIMENTAL SECTION

**Chemistry.** All of the solvents and reagents were obtained commercially and used without further purification. The progress of all of the reactions was monitored by TLC on precoated silica gel 60 F254 plates of thickness 0.25 mm (Merck). The chromatograms were

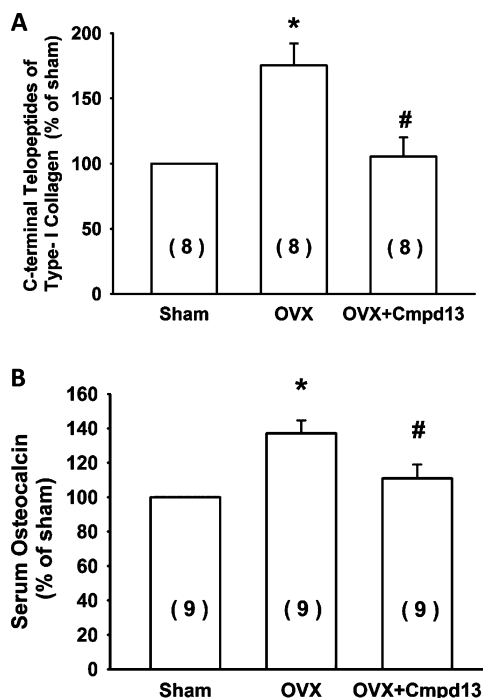


**Figure 6.** Compound 13 antagonizes OVX-induced change of serum levels of bone resorption and bone formation markers. Female mice were ovariectomized. Mice were then sacrificed 4 weeks after ovariectomy, and the serum was collected. (A) Determination of C-terminal telopeptides of type-I collagen (CTx) in serum using a RatLaps EIA kit ( $N = 8$ ). (B) Determination of osteocalcin in serum using a Rat-MID osteocalcin EIA kit ( $N = 9$ ). Note that OVX increased both serum markers of CTx and osteocalcin, which was antagonized by compound 13 (Cmpd 13) treatment. Data are presented as the mean  $\pm$  SEM, \*,  $p < 0.05$  as compared with Sham. #,  $p < 0.05$  as compared with the OVX group.

visualized under UV 254–366 nm. The following adsorbant was used for column chromatography: silica gel 60 (Merck, particle size 0.063–0.200 mm). NMR spectra were obtained on a Bruker Avance III 500 FT-NMR spectrometer in  $CDCl_3$ . High resolution MS spectra were measured either in the instruments center of National Chung Hsing University (JEOL JMS-700 spectrometer) or National Tsing Hua University (FINNIGAN, MAT-95XL HRMS). All tested compounds have above 95% purity by HPLC using a Shimadzu LC-20AT system and a photodiode array detector SPD-M-20A. The NMR spectra of all known compounds have NMR data identical to the reported compounds.

**1-Benzyl-3-(5'-ethenylfuran-2'-yl)indazole (3).** To the solution of methyltriposphonium bromide (714 mg, 2 mmol) in anhydrous THF (4 mL), *t*-BuOK (225 mg, 2 mmol) was added, and the solution was turned to yellow. After 10 min, 5-(1-benzyl-1H-indazol-3-yl)furan-2-carbaldehyde (300 mg, 1 mmol) in anhydrous THF (2 mL) was added to the previous solution. After the reaction was completed, saturated ammonia chloride solution was added to stop the reaction. THF was evaporated, and the mixture was partitioned with  $CH_2Cl_2$ , washed with brine, and dried over  $MgSO_4$ . The desired compound was obtained by flash chromatography using a hexane–EtOAc system (37% yield, orange oil).  $^1H$  NMR (200 Hz,  $CDCl_3$ )  $\delta$  8.13(d,  $J = 8$  Hz, 1H), 7.15–7.40 (m, 8H), 6.90 (d,  $J = 3.4$  Hz, 1H), 6.59 (dd,  $J = 11.0, 17.0$  Hz, 1H), 6.41 (d,  $J = 3.4$  Hz, 1H), 5.81 (d,  $J = 17.0$  Hz, 1H), 5.62 (s, 2H), 5.22 (d,  $J = 11.0$  Hz, 1H). HRMS [ESI]<sup>+</sup> calculated for  $C_{20}H_{16}N_2O$  300.1263; found  $[M - 1]^+$  299.0688.

**1-Benzyl-3-(5'-ethoxyfuran-2'-yl)-1H-indazole (4).** Hydroboration–oxidation was performed to obtain the desired compound. To the solution containing 3 (243 mg, 0.81 mmol) in anhydrous THF (6 mL) at 0 °C under inert atmosphere, 0.81 mL of borane dimethyl sulfide complex solution (2 M in THF) was added. After 3 h, sodium

hydroxide solution [421 mg in EtOH/H<sub>2</sub>O (65/32)] followed by hydrogen peroxide (30% wt, 2 mL) was added, and the reaction was stopped after 4 h. The mixture was partitioned with water and dichloromethane and dried over MgSO<sub>4</sub>. The desired compound was obtained by flash chromatography using a hexane–EtOAc system (7% yield, colorless amorphous). <sup>1</sup>H NMR (200 Hz, CDCl<sub>3</sub>) δ 8.01 (*d*, *J* = 8.0 Hz, 1H), 7.14–7.33 (*m*, 8H), 6.83 (*d*, *J* = 3.2 Hz, 1H), 6.28 (*d*, *J* = 3.2 Hz, 1H), 5.62 (*s*, 2H), 3.97 (*t*, *J* = 6.2 Hz, 2H), 3.03 (*t*, *J* = 6.2 Hz, 2H). HRMS [ESI]<sup>+</sup> calculated for C<sub>20</sub>H<sub>18</sub>N<sub>2</sub>O<sub>2</sub> 318.1368; found [M + 1]<sup>+</sup> 319.1441.

**tert-Butyl 5-(1-benzyl-1H-indazol-3-yl)furan-2-carboxylate (10).** To a solution of *tert*-BuOH (0.03 mL, 0.3 mmol), DCC (49 mg, 0.23 mmol), and DMAP (29 mg, 0.23 mmol) in dichloromethane, compound 8 (50 mg, 0.16 mmol) was added and stirred overnight. Water and 1 N HCl solution were added, and the mixture was partitioned with dichloromethane three times, washed with brine, and dried over MgSO<sub>4</sub>. The residue was subjected to flash chromatography using a hexane–EA system (16% yield, colorless amorphous). <sup>1</sup>H NMR (400 Hz, CDCl<sub>3</sub>) δ 8.27 (*d*, *J* = 7.8 Hz, 1H), 7.19–7.35 (*m*, 9H), 6.98 (*d*, *J* = 7.6 Hz, 1H), 5.63 (*s*, 2H), 1.23 (*s*, 9H). HRMS [ESI]<sup>+</sup> calculated for C<sub>23</sub>H<sub>22</sub>N<sub>2</sub>O<sub>3</sub> 374.1630; found [M+1]<sup>+</sup> 375.1704.

**5-(1-Benzyl-1H-indazol-3-yl)-N-methoxy-N-methylfuran-2-carboxamide (11).** To a solution of compound 8 (955 mg, 3 mmol) in 5 mL of anhydrous CH<sub>2</sub>Cl<sub>2</sub>, one drop of DMF was added to increase solubility, and oxalyl chloride (2.54 mL, 30 mmol) was added slowly at 0 °C and inert atmosphere for 30 min. Excess oxalyl chloride was removed. Anhydrous CH<sub>2</sub>Cl<sub>2</sub> (10–15 mL) was added to the residue, and 2-dimethylaminoethanol (1 mL, 10 mmol) was added and stirred overnight. After the usual workup, the residue was subjected to flash chromatography using a dichloromethane–methanol system (47% yield, light yellow, oily). <sup>1</sup>H NMR (200 Hz, CDCl<sub>3</sub>) δ 8.07 (*d*, *J* = 8.2 Hz, 1H), 7.17–7.36 (*m*, 9H), 6.96 (*d*, *J* = 3.3 Hz, 1H), 5.62 (*s*, 2H), 3.53 (*dd*, *J* = 5.8, 12.0 Hz, 2H), 2.56 (*t*, *J* = 6.0 Hz, 2H), 2.32 (*s*, 6H). HRMS [ESI]<sup>+</sup> calculated for C<sub>23</sub>H<sub>23</sub>N<sub>3</sub>O<sub>3</sub> 389.1739; found [M]<sup>+</sup> 389.1731.

**2-(Dimethylamino)ethyl 5-(1-benzyl-1H-indazol-3-yl)furan-2-carboxylate (13).** To a solution containing compound 8 (955 mg, 3 mmol) in CH<sub>2</sub>Cl<sub>2</sub> (5 mL) and several drops of DMF and 1,1'-carbonyldiimidazole (CDI, 648 mg, 4 mmol) were added slowly. After CO<sub>2</sub> release, *N,O*-dimethylhydroxylamine (244 mg, 4 mmol) was added and stirred overnight. Water was added to stop the reaction. After partitioning with dichloromethane and drying over MgSO<sub>4</sub>, the residue was subjected to flash chromatography to get the desired compound (25% yield, colorless, amorphous). <sup>1</sup>H NMR (200 Hz, CDCl<sub>3</sub>) δ 8.31 (*d*, *J* = 8.0 Hz, 1H), 7.20–7.34 (*m*, 9H), 7.00 (*d*, *J* = 3.6 Hz, 1H), 5.62 (*s*, 2H), 3.80 (*s*, 3H), 3.39 (*s*, 3H). HRMS [ESI]<sup>+</sup> calculated for C<sub>21</sub>H<sub>19</sub>N<sub>3</sub>O<sub>3</sub> 361.1426; found [M]<sup>+</sup> 361.1422.

**Methyl 5-(1-benzyl-1H-indazol-3-yl)-3-methylfuran-2-carboxylate (14).** To a solution of benzyl chloride (10 g, 71.4 mmol) in CH<sub>2</sub>Cl<sub>2</sub> (50 mL) and ClCH<sub>2</sub>CH<sub>2</sub>Cl (50 mL), methyl 3-methyl-2-furoate (5 g, 35.7 mmol) and anhydrous ferric chloride (5 g, 30.8 mmol) were added. The reaction mixture was then heated under refluxing for 2 h, cooled, and quenched with water to stop the reaction. After partitioning with dichloromethane and drying over MgSO<sub>4</sub>, the residue was subjected to flash chromatography to the corresponding ketone (1.75 g, 20% yield). The intermediate (1.19 g, 4.87 mmol) was refluxed with sodium acetate (804 mg, 9.79 mmol) and hydrazine-2HCl (3.05 g, 15.64 mmol) in MeOH for 5 h. MeOH was removed by a vacuole. Water was added, and then, the mixture was partitioned with DCM. Silica gel was applied to get the imine intermediate (537 mg, 31% yield). The intermediate was dissolved in 50 mL of dichloromethane and added to the solution containing lead tetraacetate (2.0 g, 4.63 mmol) and boron trifluoride diethyl etherate (8 mL) at 0 °C and allowed to go through the cyclization reaction for 30 min. When the reaction was completed, the reaction mixture was poured into ice water to stop the reaction and then was extracted with dichloromethane. The organic layer was recovered, washed with water, 5% sodium carbonate solution until neutral, dried over MgSO<sub>4</sub>, and filtered. The solvent of the filtrate was evaporated under reduced pressure, and the residue was purified by column chromatography

(silica gel, dichloromethane/*n*-hexane = 2:1) to give the final product (177 mg, 33% yield, colorless amorphous). <sup>1</sup>H NMR (200 Hz, CDCl<sub>3</sub>) δ 7.98–8.02 (*m*, 2H), 7.2–7.43 (*m*, 8H), 5.47 (*s*, 2H), 3.90 (*s*, 3H), 2.30 (*s*, 3H). HRMS [ESI]<sup>+</sup> calculated for C<sub>21</sub>H<sub>18</sub>N<sub>2</sub>O<sub>3</sub> 346.1317; found [M + 1]<sup>+</sup> 347.1391.

**5-(1-Benzyl-1H-indazol-3-yl)-3-methylfuran-2-carboxylic Acid (15).** Compound 14 was refluxed in MeOH and KOH<sub>(aq)</sub> until it disappeared. The solvent was evaporated, and 1 N HCl aqueous solution was added. Dichloromethane and ethyl acetate were used for partitioning. <sup>1</sup>H NMR (200 Hz, CH<sub>3</sub>OH-*d*<sub>4</sub>) δ 8.04 (*d*, *J* = 3.2 Hz, 1H), 7.24–7.50 (*m*, 8H), 5.57 (*s*, 2H), 2.38 (*s*, 3H). HRMS [ESI]<sup>+</sup> calculated for C<sub>20</sub>H<sub>16</sub>N<sub>2</sub>O<sub>3</sub> 332.1161; found [M]<sup>+</sup> 332.1167.

**Materials for Biological Studies.** Recombinant mouse RANKL (462-TEC: amino acids 158–317 expressed in *Escherichia coli*) and mouse M-CSF were purchased from R&D System (Minneapolis, MN, USA). RANKL and M-CSF were stored in –20 °C. Tartrate resistant acid phosphatase (TRAP) staining kit, 3-(4,5-dimethylthiazol-2-yl)-2,5-diphenyltetrazolium bromide (MTT), β-glycerophosphate, and L-ascorbic acid were obtained from Sigma-Aldrich (St. Louis, MO, USA). Alendronate was from Calbiochem. α-MEM was from Gibco Invitrogen (Carlsbad, CA, USA). Fetal bovine serum was from Biological Industries (Kibbutz Beit Haemek, Israel). A murine monocytic cell line, RAW264.7, was obtained from American Type Culture Collection (Manassas, VA). Rabbit polyclonal antibody for IKKα/β, phosphor-IKKα/β, phosphor-NFκB p65, NFκB p65, and goat anti-mouse or anti-rabbit secondary antibody conjugated with horseradish peroxidase were from Santa Cruz Biotechnology (Santa Cruz, CA, USA). Mouse monoclonal antibody for actin was from Merck-Millipore (Bedford, MA, USA).

**Osteoclastogenesis.** Bone marrow cells derived from tibiae and femurs of 8–10 week old male Sprague–Dawley rats or ICR mice were cultured with α-MEM. After incubation for 24 h, the hematopoietic cells (nonadherent cells) were collected and plated at 10<sup>6</sup> cells/well in 24 wells in the presence of RANKL (50 ng/mL), M-CSF (20 ng/mL), and the testing compounds for 5 days. After 5 days, the cells were fixed in PBS containing 4% paraformaldehyde. Osteoclast formation was confirmed by TRAP staining. Cells were then treated with the TRAP staining kit (70 μg/mL Fast Garnet GBC base solution, 125 μg/mL naphthol AS-B1 phosphoric acid, 100 mM acetate, and 6.7 mM tartrate) at 37 °C for 1 h. Both TRAP-positive and nuclei ≥3 were counted as osteoclasts.

**Resorption Assay.** Bone marrow-derived preosteoclasts from male rats were seeded at 10<sup>6</sup> cells/well in Osteo Assay Plate 24 wells (Corning, USA) in the presence of 50 ng/mL RANKL and 20 ng/mL M-CSF for 5 days. After 5-days' culture, RANKL and M-CSF were then removed, and the testing compound was added for another 3 days. The wells were washed with 1 N sodium hydroxide solution to remove the cells. The resorbed areas on the wells were photographed with an inverted microscope (Olympus 4J18950-DP70, Tokyo, Japan) and were quantified using ImageJ software, version 1.48 (US National Institutes of Health, Bethesda, MD, USA).

**3-(4,5-Dimethylthiazol-2-yl)-2,5-diphenyltetrazolium Bromide (MTT) Assay.** Bone marrow-derived preosteoclasts (non-adherent cells) were seeded at 10<sup>6</sup> cells/well in 24 wells in the presence of 20 ng/mL M-CSF for 3 days. After 3 days' culture, the testing compound was added for another 5 days. After washing, 200 μL of α-MEM containing 0.5 mg/mL of MTT was added to each well. Cells were incubated at 37 °C for 60 min. The blue crystals formed in viable cells were solubilized with 500 μL of DMSO. The absorbance of each well was measured at 550 nm. Osteoblasts were plated in 24 wells for 24 h and then added with different testing compounds for another 24 h. After washing, 200 μL of α-MEM containing 0.5 mg/mL of MTT was added to each well. Cell viability was assayed as mentioned above.

**Bone Nodule Formation.** Cranium cultured cells (preosteoblasts) were seeded in 24 wells and cultured with α-MEM containing 10% FBS. Ten millimolar β-glycerophosphate and 50 μg/mL L-ascorbic acid were then added in the presence or absence of testing compounds for 2 weeks to form the bone mineralized nodule. After 2 weeks, the cells were fixed in ice-cold 75% (v/v) ethanol for 30 min and stained

with 40 mM alizarin red solution (pH 4.2). The alizarin red-S in samples was quantified by measuring absorbance at 550 nm and calculated according to a standard curve.

**Ovariectomy-Induced Osteoporosis.** All protocols complied with institutional guidelines and were approved by the Animal Care Committees of Medical College, National Taiwan University. Twelve week old female ICR mice were used in the animal study. Mice were ovariectomized bilaterally under isoflurane anesthesia, and control mice were sham-operated for comparison. Mice were all kept under controlled conditions at room temperature ( $22 \pm 1$  °C) and a 12 h light–dark cycle. The body weights of mice were recorded weekly. Compound 13 was administered (s.c.) at 10 mg/kg, 5 days/week for 30 days.

**Western Blot.** RAW264.7 cells were plated in 6 wells. After reaching confluence, cells were incubated with compound 13 (10  $\mu$ M) for 2 h and treated with RANKL (50 ng/mL) for different time intervals. Cells were then washed with cold PBS and lysed for 30 min at 4 °C with lysis buffer as described previously.<sup>3</sup> Equal protein (30  $\mu$ g) was applied per lane, and electrophoresis was performed under denaturing conditions on a 10% SDS gel and transferred to an immobilon-P (PVDF) membrane (Merck-Millipore, Bedford, MA, USA). The blots were blocked with 5% nonfat milk in TBS-T (0.5% Tween 20 in 20 mM Tris and 137 mM NaCl) for 1 h at room temperature and then probed with antibodies against specific antigens (1:1,000) at 4 °C overnight. After three washes by TBS-T, the blots were subsequently incubated with goat anti-rabbit or anti-mouse peroxidase-conjugated secondary antibody (1:10,000) for 1 h at room temperature. The blots were visualized by enhanced chemiluminescence using Amersham Hyperfilm ECL (GE Healthcare, Upland, CA, USA) or Biospectrum Imaging System (UVP, Upland, CA, USA).

**Microcomputed Tomography ( $\mu$ CT) Analysis.** Tibiae were removed from mice on day 30 and fixed by 4% paraformaldehyde, and  $\mu$ CT analysis was then performed. Fixed bones were subjected to X-ray microtomography by using Skyscan 1076 (SKYSCAN, Kontich, Belgium). Scanning was done at 40 kV and 600  $\mu$ A, and the rotation step was 0.3° per image. The images were collected at a resolution of 9  $\mu$ m/pixel for isolated tibiae. Reconstruction of sections was carried out with a GPU-based scanner software (GPU-NRecon). Quantification of trabecular bone morphometric indexes was performed 0.5–1.5 mm distal to the growth plate of the proximal ends of tibia. The analysis was performed by scanner software (CTAn). Trabecular morphology was described by measuring bone volume fraction (bone volume/tissue volume, BV/TV), trabecular number (Tb.N), and trabecular thickness (Tb.Th). The 3D images were obtained with scanner software (CTvox).

**Bone Histomorphometry.** Tibiae were removed from mice on day 30 and fixed by 4% paraformaldehyde at 4 °C for 48 h. Tibiae were then decalcified with 10% Na<sub>2</sub>EDTA at 4 °C for 14 days, dehydrated in increasing concentrations of ethanol, and embedded in paraffin. The serial histological sections were cut longitudinally (4  $\mu$ m) and stained with Meyer's hematoxylin–eosin solution.

**Measurement of the Serum Levels of Bone Resorption and Bone Formation Markers.** Mice were sacrificed on day 30 after ovariectomy, and blood samples were collected for the preparation of serum samples. Serum samples were prepared by centrifuging blood (1500g for 15 min) with vacutainer tubes (Becton Dickinson, Franklin lakes, NJ, USA). C-Terminal telopeptides of type-I collagen (CTx), a bone resorption marker, in serum was determined by using a RatLaps EIA kit, and osteocalcin, a bone formation marker, in serum was evaluated by using a Rat-MID osteocalcin EIA kit. ELISA kits were all from Immunodiagnostic Systems Ltd. (Baldon Colliery, Tyne & Wear, United Kingdom).

## ■ ASSOCIATED CONTENT

### Ⓢ Supporting Information

Compound 13 has no inhibition of osteoblast and MTT results. The Supporting Information is available free of charge on the ACS Publications website at DOI: 10.1021/jm502014h.

## ■ AUTHOR INFORMATION

### Corresponding Authors

\*(W.-M.F.) Tel: +886-2-23123456, ext. 88319. E-mail: wenmei@ntu.edu.tw.

\*(H.-Y.H.) Tel: +886-6-2353535, ext. 6803. E-mail: z10308005@email.ncku.edu.tw.

### Notes

The authors declare no competing financial interest.

## ■ ACKNOWLEDGMENTS

The investigation was supported by research grants from Ministry of Science and Technology of Republic of China (MOST 103-2320-B-006-046-MY2) awarded to H.-Y.H.

## ■ ABBREVIATIONS USED

OVX, ovariectomized; RANKL, receptor activator of nuclear factor kappa-B ligand; M-CSF, macrophage colony-stimulating factor; RANK, receptor activator of nuclear factor kappa-B; NF- $\kappa$ B, nuclear factor kappa-B; NO, nitric oxide; BMD, bone mineral density; sGC, soluble guanylyl cyclase; cGMP, cyclic guanosine monophosphate; TRAP-stain, tartrate resistant acid phosphatase-stain; BV/TV %, trabecular bone volume relative to the tissue volume; Tb.N, trabecular bone number; Tb.Th, trabecular thickness; CTx, C-terminal telopeptides of type-I collagen

## ■ REFERENCES

- (1) Dawson-Hughes, B.; Looker, A. C.; Tosteson, A. N.; Johansson, H.; Kanis, J. A.; Melton, L. J., III. The potential impact of the National Osteoporosis Foundation guidance on treatment eligibility in the USA: an update in NHANES 2005–2008. *Osteoporosis Int.* **2012**, *23*, 811–820.
- (2) Burge, R.; Dawson-Hughes, B.; Solomon, D. H.; Wong, J. B.; King, A.; Tosteson, A. Incidence and economic burden of osteoporosis-related fractures in the United States, 2005–2025. *J. Bone Miner. Res.* **2007**, *22*, 465–475.
- (3) Cooper, C.; Cole, Z. A.; Holroyd, C. R.; Earl, S. C.; Harvey, N. C.; Dennison, E. M.; Melton, L. J.; Cummings, S. R.; Kanis, J. A.; IOF CSA Working Group on Fracture Epidemiology. Secular trends in the incidence of hip and other osteoporotic fractures. *Osteoporosis Int.* **2011**, *22*, 1277–1288.
- (4) Modi, A.; Sajjan, S.; Gandhi, S. Challenges in implementing and maintaining osteoporosis therapy. *Int. J. Women's Health* **2014**, *6*, 759–769.
- (5) Roman-Garcia, P.; Quiros-Gonzalez, I.; Mottram, L.; Lieben, L.; Sharan, K.; Wangwatsin, A.; Tubio, J.; Lewis, K.; Wilkinson, D.; Santhanam, B.; Sarper, N.; Clare, S.; Vassiliou, G. S.; Velagapudi, V. R.; Dougan, G.; Yadav, V. K. Vitamin B<sub>12</sub>-dependent taurine synthesis regulates growth and bone mass. *J. Clin. Invest.* **2014**, *124*, 2988–3002.
- (6) Wu, K.; Lin, T. H.; Liou, H. C.; Lu, D. H.; Chen, Y. R.; Fu, W. M.; Yang, R. S. Dextromethorphan inhibits osteoclast differentiation by suppressing RANKL-induced nuclear factor-kappaB activation. *Osteoporosis Int.* **2013**, *24*, 2201–2214.
- (7) Kohli, S. S.; Kohli, V. S. Role of RANKL-RANK/osteoprotegerin molecular complex in bone remodeling and its immunopathologic implications. *Indian J. Endocrinol. Metab.* **2011**, *15*, 175–181.
- (8) Yavropoulou, M. P.; Yovos, J. G. Osteoclastogenesis—current knowledge and future perspectives. *J. Musculoskeletal Neuronal Interact.* **2008**, *8*, 204–216.
- (9) Ross, F. P. M-CSF, c-Fms, and signaling in osteoclasts and their precursors. *Ann. N.Y. Acad. Sci.* **2006**, *1068*, 110–116.
- (10) Maeda, S. S.; Lazaretti-Castro, M. An overview on the treatment of postmenopausal osteoporosis. *Arq. Bras. Endocrinol. Metabol.* **2014**, *58*, 162–171.

- (11) Jamal, S. A.; Hamilton, C. J. Nitric oxide donors for the treatment of osteoporosis. *Curr. Osteoporosis Rep.* **2012**, *10*, 86–92.
- (12) Jamal, S. A.; Reid, L. S.; Hamilton, C. J. The effects of organic nitrates on osteoporosis: a systematic review. *Osteoporosis Int.* **2013**, *24*, 763–770.
- (13) Friebe, A.; Koesling, D. Mechanism of YC-1-induced activation of soluble guanylyl cyclase. *Mol. Pharmacol.* **1998**, *53*, 123–127.
- (14) Collot, V.; Dallemagne, P.; Bovy, P. R.; Rault, S. Suzuki-type cross-coupling reaction of 3-iodoindazoles with aryl boronic acids: A general and flexible route to 3-arylindazoles. *Tetrahedron* **1999**, *55*, 6917–6922.
- (15) Lien, J. C.; Lee, F. Y.; Huang, L. J.; Pan, S. L.; Guh, J. H.; Teng, C. M.; Kuo, S. C. 1-Benzyl-3-(5'-hydroxymethyl-2'-furyl)indazole (YC-1) derivatives as novel inhibitors against sodium nitroprusside-induced apoptosis. *J. Med. Chem.* **2002**, *45*, 4947–4949.
- (16) An, H.; Kim, N.-J.; Jung, J.-W.; Jang, H.; Park, J.-W.; Suh, Y.-G. Design, synthesis and insight into the structure–activity relationship of 1,3-disubstituted indazoles as novel HIF-1 inhibitors. *Bioorg. Med. Chem. Lett.* **2011**, *21*, 6297–6300.
- (17) Lee, F. Y.; Lien, J. C.; Huang, L. J.; Huang, T. M.; Tsai, S. C.; Teng, C. M.; Wu, C. C.; Cheng, F. C.; Kuo, S. C. Synthesis of 1-benzyl-3-(5'-hydroxymethyl-2'-furyl)indazole analogues as novel anti-platelet agents. *J. Med. Chem.* **2001**, *44*, 3746–3749.
- (18) Chou, L. C.; Huang, L. J.; Hsu, M. H.; Fang, M. C.; Yang, J. S.; Zhuang, S. H.; Lin, H. Y.; Lee, F. Y.; Teng, C. M.; Kuo, S. C. Synthesis of 1-benzyl-3-(5-hydroxymethyl-2-furyl)selenolo[3,2-c]pyrazole derivatives as new anticancer agents. *Eur. J. Med. Chem.* **2010**, *45*, 1395–1402.
- (19) Wang, H.; Liu, J.; Yin, Y.; Wu, J.; Wang, Z.; Miao, D.; Sun, W. Recombinant human parathyroid hormone related protein 1–34 and 1–84 and their roles in osteoporosis treatment. *PLoS One* **2014**, *9*, e88237.